2020년 2월
석사학위 논문

Spiropyran Derivatives as a Photosensitizer for Photoswitchable ROS Generation

조 선 대 학 교 대 학 원

화 학 과

박 세 영

Spiropyran Derivatives as a Photosensitizer for Photoswitchable ROS Generation

2020년 2월 25일

조 선 대 학 교 대 학 원

화 학 과

박 세 영

Spiropyran Derivatives as a Photosensitizer for Photoswitchable ROS Generation

지도교수 이 종 대

논문을 이학석사학위신청 논문으로 제출함.

2020년 2월

조 선 대 학 교 대 학 원

화 학 과

박 세 영

박세영의 석사학위논문을 인준함

위원장 조선대학교 교수 손 홍 래 (인)

위 원 조선대학교 교수 김 호 중 (인)

위 원 조선대학교 교수 이 종 대 (인)

2020년 2월

조 선 대 학 교 대 학 원

TABLE OF CONTENTS

TABLE OF CONTENTS i
LIST OF FIGURES ii
LIST OF TABLE iii
LIST OF SCHEMES iv
ABSTRACT 1

Spiropyran Derivatives as a Photosensitizer for Photoswitchable ROS Generation

1. Introduction

2. Experimental Section

3. Results and Discussion

4. Conclusion

5. References

LIST OF FIGURES

Figure 1

Figure 2

Figure 3

Figure 4

Figure 5

Figure 6

Figure 7

LIST OF TABLES

Table 1

No.	closed form
1	10.00
2	11.16
3	11.21
4	10.56
5	10.85
6	12.87

Table 1. Predicted log P Values of Spiropyran of **1** − **6**[a]

LIST OF SCHEMES

Scheme 1

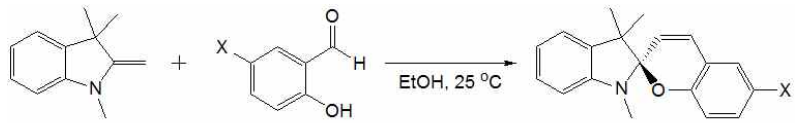

X = H **1**, Br **2**, NO_2 **3**

Scheme 2

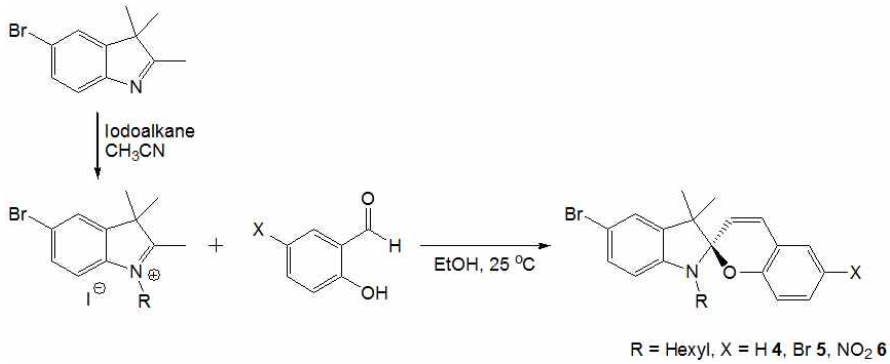

R = Hexyl, X = H **4**, Br **5**, NO_2 **6**

ABSTRACT

Spiropyran Derivatives as a Photosensitizer for Photoswitchable ROS Generation

So Young Ma, Se-Young Park, Jong-Dae Lee*

Department of Chemistry, College of Natural Sciences, Chosun University, 309 Pilmundaero, Dong-gu, Gwangju 61452, South Korea

Keywords: Spiropyran; Photodynamic therapy; Reactive oxygen species; singlet oxygen; cancer cell

Reversibly controlled generation of singlet oxygen from photosensitizing materials benefits in selective cell killing and controllable effect time, but is a challenging option for photodynamic therapies. A series of new spiropyrans of indoline series with N-alkylation has been synthesized, their structure and photochromic properties have been studied. The structure of the obtained compounds was confirmed by the data of ^{1}H, ^{13}C NMR, IR spectroscopy, and elemental analysis. Photochromic properties of the prepared compounds have been studied. We found spiropyran derivatives have photoswitching properties in both fluorescence and singlet oxygen generation in aqueous solutions and cells, and demonstrated N-alkylated spiropyrans enhanced photosensitization and emission could be potentially applied for photodynamic therapy studies on tumor cells.

1. INTRODUCTION

Photochromic compounds undergo unimolecular, bidirectional reversible structural and chemical changes after irradiation with light. If applied correctly, light can be operated as a harmless and selective external trigger to control material properties or even biological processes if the target photo-switch is soluble in aqueous solution. In contrast to azobenzenes[1－8] which undergo photo-induced cis/trans isomerization, spiropyrans,[9－12] diarylethenes,[13] fulgides[14－16] and fulgimides[17,18] exist in an open-ring and closed isomeric form. Spiropyrans possess an indoline and a chromene moiety and can be switched reversibly between the closed-ring, nonpolar spiropyran **(SP)** structure and the open-ring merocyanine **(MC)** which adopts a zwitterionic or a quinoidal mesomeric resonance structure. Furthermore, **MC** is known to exist as different cis (C) / trans (T) isomers due to its central ethylene bridge (Chart 1) with the two adjacent bonds. In principle eight different conformations are imaginable, but due to steric reasons only those four with trans conformation in the middle are stable.[12]

The corresponding main absorption bands of both photoisomers are well separated and typically account for a yellow **SP** and a reddish **MC** form. The photochromic features as well as the thermodynamically favored state considerably depend on the particular substituents attached to the indoline and chromene moieties.

Spiropyrans are widely used in material sciences[19－21] and thus, have been subjected to numerous experimental steady-state and also ultrafast time-resolved studies in organic solvents.[10,22－24] Moreover, theoretical studies have been carried out[25,26] also under simulation of aqueous conditions.[27] Since spiropyrans are getting more and more into the focus for the control of biological systems,[28－30] it is necessary to understand their switching behavior and photodynamics in aqueous conditions thoroughly, as these features may differ significantly because of the increased solute polarity. The obtained results could help tuning the photo-responsive properties to design enhanced spiropyran photoswitches for diverse applications.

The best studied and mostly applied spiropyran derivative is the nitro-substituted

1',3',3'-trimethylspiro[2H-1-benzopyran-2,2-indoline], which has been introduced to various biological environments like RNA,[28] DNA,[31] and proteins so far.[32] NO_2-substituted spiropyran has been found to undergo hydrolysis under aqueous conditions[33－35] and shows loss of switching efficiency in the presence of DNA.[36]

As part of our ongoing research into the utility of the *N*-alkylated spiropyran chemistry, we have published preliminary data on spiropyran derivatives.[37] Here, we give the full details of the synthesis, characterization, and biological activity of the *N*-alkylated spiropyrans, which involve hydrogen, bromide, and nitro group substituents in chromene unit.

We synthesized N-alkylated H- (1), Br- (2) and NO2-substituted spiropyran (3) derivatives on the indolene ring (Scheme 1). The photophysical properties should give important evidence about the influence of the chromene part on the photochromic behavior of spiropyrans in aqueous conditions. Hence, we performed photoswitching and thermal relaxation studies as well as fluorescence measurements in order to characterize the steady state properties of the most promising spiropyrans.

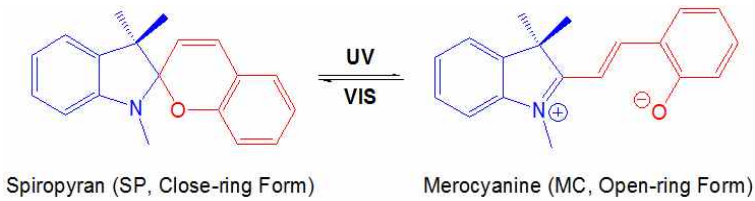

Spiropyran (SP, Close-ring Form) Merocyanine (MC, Open-ring Form)

Chart 1. Reversible photochromic reaction between the closed spiropyran **(SP)** and the open-ring merocyanine **(MC)** isomer of the spiropyran compound.

2. EXPERIMENTAL

2.1. General considerations

All manipulations were performed under either a dry nitrogen atmosphere using either standard Schlenk techniques. Ethanol, and acetic acid were purchased from Samchun Pure Chemical Company and used without further purification. Acetonitrile was dried over sodium/benzophenone before use. Glassware, syringes, magnetic stirring bars, and needles were dried overnight in a convection oven. Salicylic aldehyde, 4-nitrosalicylic aldehyde, 4-bromosalicylic aldehyde, 4-bromonitrobenzene, 1,3,3-trimethyl-2-methyleneindoline, sodium nitrite, tin (II) chloride dihydrate, 3-methylbut-2-one, iodoalkane were purchased from Aldrich Chemicals. All compounds were synthesized by modified literature procedure.[37] IR spectra were recorded on an Agilent Cary 600 Series FT-IR spectrometer using KBr disks. The ^{1}H and ^{13}C NMR spectra were recorded on a Bruker 300 spectrometer operating at 300.1 and 75.4 MHz, respectively. All ^{1}H and ^{13}C NMR chemical shifts were measured relative to the internal residual $CHCl_3$ from the lock solvent (99.9% $CDCl_3$). Elemental analyses (Carlo Erba Instruments CHNS-O EA1108 analyzer) were performed by the Ochang branch of the Korean Basic Science Institute. All melting points were uncorrected.

2.2. Cell Culture and Observation

Ba/F3 murine IL-3-dependent pro-B cell line, Jurkat human T cell leukemic and HeLa human epithelial carcinoma were purchased from KRIBB BioResource Center. Enhanced green fluorescent protein (EGFP)-expressing Ba/F3 cells were kindly gifted from Prof. Hiroyuki Nakamura (The University of Tokyo). RPMI-1640 medium was from Wako Pure Chemicals. Fetal bovine serum was purchased from Thermo Fisher Scientific.

2.3. In Vitro Cytotoxicity Evaluation

The cytotoxicity of compounds **3** − **6** to C6 glioma cell line (rat brain cancer cell) was

assessed by the MTT cell viability assay. In summary, C6 glioma cells were seeded into a 96-well microplate at a density of 5 × 10^4cells/well in 100 μL of Ham's F-12 medium, supplemented with 10% fetal bovines erum(FBS), and allowed to adhere overnight at 37°C in 5% CO_2. The medium was then replaced with the same volume of Ham's F-12 containing different concentrations (0−10 μM) of compounds **3** − **6** and afterward, cytotoxicity was assessed in 2 h incubation at 37 °C for 4 h in the dark after addition of compounds **3** − **6**. Then, the cells were washed twice with PBS, and 100 μL of MTT (5 mg/mL in PBS) was added to each well and the plates were incubated at 37 °C for 4 h in the dark. The medium was removed and 200 μL of DMSO was added to dissolve the blue formazan crystals for 20 min. The absorbance was read on an ELISA Reader at 540 nm. The relative cell viability was calculated by dividing the mean optical density value of the control group, and the average value was obtained from six parallel samples. The effect of UV irradiation was investigated after treating of C6 glioma cells with the aforementioned compounds in a range of concentrations from 0 to 10 μM for 2 h at 37 °C in 5% CO_2 and then exposing them to UV lamp (365nm) with a 10 cm distance for 3 min. Immediately after UV irradiation and illumination with greenligh (532nm) for 90 s, the cell viability was measured using the technique mentioned before. All experiments were performed in triplicate.

2.4. Intracellular ROS Detection

ROS amounts were evaluated by a fluorescent probe (DCFH) to detect ROS generation rate as a commonly employed fluorescent detection method, and this fluorescent probe was obtained by activation of DCFH-DA.[38] C6 cells were cultured in Ham's F-12 medium (10% FBS), trypsinized, counted, and re-suspended in fresh complete media at a density of 3 × 10^4cells/mL. Next, they were seeded into 24-well plates and incubated for 24 h at 37 °C, and then were treated with 0.01μM of the compounds **3** − **6** in PBS. After 2 h incubation period, the cells were loaded with an ROS detector probe by replacing the culture media with PBS, containing 5 μM DCFH-DA for 30 min at 37 °C in dark, and non-incorporated DCFH-DA was removed through washing with PBS three times. Afterward, half of the wells were exposed to UV irradiation (365 nm, 12 W) at a distance

of 10 cm for 3 min and then illuminated with a green light at 532 nm for 90 s. Fluorescence emissions at 530 nm (excitation at 485 nm) were measured at 1 min intervals for a total of 5 min. In each analysis, two types of control sample were used: negative control (non-UV irradiated cells) and positive control (UV-irradiated cells at 365 nm).

2.5. Synthesis of spiropyran derivatives (**1** − **3**)

General Procedure. 1,3,3-Trimethyl-2-methyleneindoline (3.47 g, 20.0 mmol) and 1.2 equiv of salicylic aldehyde (2.93 g, 22.0 mmol) dissolved in anhydrous ethanol (50 mL) and the mixture was stirred at 25 °C for 7 h. The progress of the reaction was monitored by thin layer chromatography. After completion of the reaction, the removal of the solvent at the rotary evaporator gave a crude product, which was then chromatographed (SiO_2, Hx : EA = 2 : 1) to yield **1**.

Characterization of N-mehtyl substituted spiropyran derivatives **1** − **3**.

1: Yield: 64% (3.55 g, 12.8 mmol). M.P. 75 − 76 °C. Elemental Analysis : $C_{19}H_{19}NO$, Found : C, 82.25; H, 6.97; N, 5.11; O, 5.83. Calcd : C, 82.28; H, 6.90; N, 5.05; O, 5.77. IR (KBr pellet, cm^{-1}) ν(C−H) 2910, ν(=C−H) 3285, ν(C=C, vinyl) 1650, ν(C=C, aromaticring) 1605, ν(C−N) 1271, ν(C−O) 1090. ^{1}H NMR ($CDCl_3$-*d*) δ 1.40 (s, 3H, CH_3), 2.85 (s, 3H, N−CH_3), 6.00 (d, 1H, =C*H*, $^3J_{C-H}$=8.5Hz), 6.82 (d, 1H,=C*H*, $^3J_{C-H}$=8.5Hz), 6.55 (d, 1H, indoline C−*H*, $^3J_{C-H}$=3.4Hz), 6.82 (m, 1H, indoline C−*H*), 7.01 (m, 1H, indoline C−*H*), 7.10 (d, 1H, indoline C−*H*, $^3J_{C-H}$=3.4Hz), 6.80 (d, 1H, chromene C−*H*, $^3J_{C-H}$=3.2Hz), 6.95 (m, 1H, chromene C−*H*), 7.15 (d, 1H, chromene C−*H*, $^3J_{C-H}$=3.2Hz), 7.25 (m, H, chromene C−*H*). ^{13}C NMR ($CDCl_3$-*d*) δ 18.0 (*C*H_3), 30.1 (N−*C*H_3), 56.1 (*C*$(CH_3)_2$), 104.1 (*C*−O), 121.1, 127.4 (=*C*−H), 112.9, 118.0, 125.7, 127.4, 134.1, 151.4 (indoline ring), 113.7, 116.6, 120.4, 129.1, 130.0, 155.3 (chromene ring).

2: Yield: 83% (5.91 g, 16.6 mmol). M.P. 80 − 81 °C. Elemental Analysis : $C_{19}H_{18}NOBr$, Found: C, 64.21; H, 5.08; N, 4.10; O, 4.54. Calcd : C, 64.06; H, 5.09; N, 3.93; O, 4.49. IR(KBr pellet, cm^{-1}) ν(C−H) 2918, ν(=C−H) 3281, ν(C=C, vinyl)1653 , ν(C=C,

aromaticring) 1604, ν(C−N) 1271, ν(C−O)1091. ^{1}H NMR ($CDCl_3$-*d*) δ 1.39 (s, CH_3), 2.87 (s, N−CH_3), 6.02 (d, =C*H*, $^{3}J_{C-H}$=8.5Hz), 6.85 (d, =C*H*, $^{3}J_{C-H}$=8.5Hz), 6.60 (d, indoline C−*H*, $^{3}J_{C-H}$=3.4Hz), 6.80 (t, indoline C−*H*, $^{3}J_{C-H}$=3.4Hz), 7.03 (t, indoline C−*H*, $^{3}J_{C-H}$=3.4Hz), 7.05 (d, indoline C−*H*, ^{3}JC−*H* = 3.4 Hz), 6.65 (d, chromene C−*H*, $^{3}J_{C-H}$=3.2Hz), 7.20 (d, chromene C−*H*, $^{3}J_{C-H}$=3.2Hz), 8.13(s, chromene C−*H*). ^{13}C NMR ($CDCl_3$-*d*) δ 18.2 (*C*H_3), 30.5 (N−*C*H_3), 55.5 (*C*(CH_3)$_2$), 104.0 (*C*−O), 121.1, 127.0 (=*C*−H), 113.0, 118.2, 125.9, 126.5, 134.1, 151.4 (indol ine ring), 114.2, 116.5, 118.2, 130.4, 135.7, 154.3 (chromene ring).

3: Yield: 88% (5.67 g, 17.6 mmol). M.P. 78 − 79 °C. Elemental Analysis : $C_{19}H_{18}N_2O_3$, Found : C, 70.81; H, 5.60; N, 8.73; O, 14.94. Calcd : C, 70.79; H, 5.63; N, 8.69; O, 14.89. IR(KBr pellet, cm^{-1}) ν(C−H)2920, ν(=C−H) 3288, ν(C=C, vinyl) 1655, ν(C=C, aromaticring) 1610, ν(C−N) 1272, ν(C−O) 1091. ^{1}H NMR ($CDCl_3$-*d*) δ 1.38 (s, CH_3), 2.85 (s,N−CH_3), 6.48 (d, =C*H*, $^{3}J_{C-H}$=8.5Hz), 6.80 (d, =C*H*, $^{3}J_{C-H}$=8.5Hz), 6.58 (d ,indoline C−*H*, $^{3}J_{C-H}$=3.4Hz), 6.82 (t, indoline C−*H*, $^{3}J_{C-H}$=3.4Hz), 7.05 (t, indoline C−*H*, $^{3}J_{C-H}$=3.4Hz), 7.08 (d, indoline C−*H*, ^{3}JC−*H* = 3.4 Hz), 7.00 (d, chromene C−*H*, $^{3}J_{C-H}$=3.2Hz), 8.05 (d, chromeneC−*H*, $^{3}J_{C-H}$=3.2Hz), 8.11 (s, chromene C−*H*). ^{13}C NMR ($CDCl_3$-*d*) δ 18.7 (*C*H_3), 30.3 (N−*C*H_3), 56.0 (*C*(CH_3)$_2$), 103.7 (*C*−O), 121.1, 127.0 (=*C*−H), 113.5, 118.0, 126.0, 126.8, 134.3, 150.7 (indoline ring), 115.1, 115.8, 120.5, 123.8, 140.6, 161.7 (chromene ring).

2.6. Synthesis of N-alkylated spiropyran derivatives (**4** − **6**)

General Procedure. 5-bromo-2,3,3-trimethyl-3H-indole was synthesized by literature procedure.[37] As shown in Scheme 2, 5-bromo-2,3,3-trimethyl-3*H*-indole (4.76 g, 20.0 mmol) was quaterinized with iodohexane (4.67 g, 22 mmol) to afford 5-bromo-1-hexyl-2,3,3-trimethyl-3*H*-indolium iodide salt. At last, N-hexylated spiropyran derivative (**4**) was obtained by Knoevenagel reaction in anhydrous ethanol (50 mL) at 25 °C for 7 h between 1.2 equiv of salicylic aldehyde (2.93 g, 22.0 mmol) and 5-bromo-1-hexyl-2,3,3-trimethyl-3*H*-indolium iodide salt (9.00 g, 20.0 mmol). The progress of the reaction was monitored by thin layer chromatography. After completion of the

reaction, the removal of the solvent at the rotary evaporator gave a crude product, which was then chromatographed (SiO_2, Hx : EA = 1 : 1) to yield **4**.

Characterization of N-alkylated spiropyran derivatives **4** − **6**.

4: Yield: 38% (3.24 g, 7.60 mmol). M.P. 94 − 96 °C. Elemental Analysis : $C_{24}H_{28}NOBr$, Found : C, 67.64; H, 6.65; N, 3.30; O, 3.81. Calcd : C, 67.60; H, 6.62; N, 3.28; O, 3.75. IR (KBr pellet, cm^{-1}) ν(C−H) 2987, ν(=C−H) 3286, ν(C=C, vinyl) 1650, ν(C=C, aromaticring) 1613, ν(C−N) 1268, ν(C−O) 1088. ^{1}H NMR ($CDCl_3$-*d*) δ 0.93 (t, 3H, $(CH_2)_5CH_3$, $^3J_{C-H}$=8.6Hz), 1.30 (m, 4H, $-CH_2-$), 1.33 (m, 2H, $-CH_2CH_3$), 1.40 (s, CH_3), 3.40 (t, 3H, N−CH_2, $^3J_{C-H}$=8.6Hz), 6.07 (d, 1H,=C*H*, $^3J_{C-H}$=8.3Hz), 6.85 (d, 1H, =C*H*, $^3J_{C-H}$=8.3Hz), 6.38 (d, 1H, indoline C−*H*, $^3J_{C-H}$=3.7Hz), 7.03 (d, 1H, indoline C−*H*, $^3J_{C-H}$=3.7Hz), 7.30 (s, 1H, indoline C−*H*), 6.77 (d, 1H, chromene C−*H*, $^3J_{C-H}$=3.5Hz), 7.00 (m, 1H, chromene C−*H*), 7.15 (d, 1H, chromene C−*H*, $^3J_{C-H}$=3.5Hz), 7.25 (m, 1H, chromene C−*H*). ^{13}C NMR ($CDCl_3$-*d*) δ 14.0, 22.5, 28.0, 28.5, 31.8, 43.5 (N-hexyl), 18.7 (CH_3), 55.5 ($C(CH_3)_2$), 101.5 (*C*−O), 121.5, 127.0 (=*C*−H), 112.4, 117.1, 129.0, 130.5, 136.7, 148.8 (indoline ring), 114.5, 116.0, 120.4, 126.8, 128.5, 155.0 (chromene ring).

5: Yield: 45% (4.55 g, 9.0 mmol). M.P. 98 − 99 °C. Elemental Analysis : $C_{19}H_{19}NO$, Found : C, 82.28; H, 6.90; N, 5.05; O, 5.77. Calcd : C, 82.28; H, 6.90; N, 5.05; O, 5.77. IR (KBr pellet, cm^{-1}) ν(C−H) 2988, ν(=C−H) 3281, ν(C=C,vinyl) 1652, ν(C=C, aromaticring) 1610, ν(C−N) 1264, ν(C−O) 1085. ^{1}H NMR ($CDCl_3$-*d*) δ 0.95 (t, 3H, $(CH_2)_5CH_3$, $^3J_{C-H}$=8.5Hz), 1.30 (m, 4H, $-CH_2-$), 1.33 (m, 2H, $-CH_2CH_3$),1.38(s, CH_3), 3.35 (t, 3H, N−CH_2, $^3J_{C-H}$=8.5Hz), 6.08 (d, 1H, =C*H*, $^3J_{C-H}$=8.3Hz), 6.89 (d, 1H, =C*H*, $^3J_{C-H}$=8.3Hz), 6.42 (d, 1H, indoline C−*H*, $^3J_{C-H}$=3.7Hz), 7.05 (d, 1H, indoline C−*H*, $^3J_{C-H}$=3.7Hz), 7.30 (s, 1H, indoline C−*H*), 6.71 (d, 1H, chromene C−*H*, $^3J_{C-H}$=3.5Hz), 7.16 (d, 1H, chromene C−*H*, $^3J_{C-H}$=3.5Hz), 8.20 (s, 1H, chromene C−*H*). ^{13}C NMR ($CDCl_3$-*d*) δ 14.1, 22.7, 27.3, 28.5, 31.5, 43.7 (N-hexyl), 18.5 (CH_3), 56.0 ($C(CH_3)_2$), 102.4 (*C*−O), 121.0, 127.2 (=*C*−H), 112.3, 118.0, 129.3, 130.7, 136.5, 148.8 (indoline ring), 114.3, 116.2, 117.2, 130.1, 132.0, 153.8 (chromene ring).

6: Yield: 52% (4.90 g, 10.4 mmol). M.P. 95 − 96 °C. Elemental Analysis : $C_{19}H_{19}NO$, Found : C, 82.28; H, 6.90; N, 5.05; O, 5.77. Calcd : C, 82.28; H, 6.90; N, 5.05; O, 5.77. IR (KBr pellet, cm^{-1}) ν(C−H) 2989, ν(=C−H) 3280, ν(C=C,vinyl) 1651, ν(C=C, aromaticring) 1609, ν(C−N) 1262, ν(C−O) 1085. ^{1}H NMR ($CDCl_3$-*d*) δ 0.96 (t, 3H, $(CH_2)_5CH_3$, $^{3}J_{C-H}$=8.7Hz), 1.28 (m, 4H, −CH_2−), 1.32 (m, 2H, −CH_2CH_3), 1.39 (s, CH_3), 3.37 (t, 3H, N−CH_2, $^{3}J_{C-H}$=8.7Hz), 6.43 (d, 1H, =C*H*, $^{3}J_{C-H}$=8.5Hz), 6.73 (d, 1H,=C*H*, $^{3}J_{C-H}$=8.5Hz), 6.42 (d, 1H, indoline C−*H*, $^{3}J_{C-H}$=3.7Hz), 7.10 (d, 1H, indoline C−*H*, $^{3}J_{C-H}$=3.7Hz), 7.30 (s, 1H, indoline C−*H*), 7.05 (d, 1H, chromene C−*H*, $^{3}J_{C-H}$=3.5Hz), 8.05 (d, 1H, chromene C−*H*, $^{3}J_{C-H}$=3.5Hz), 8.14 (s, 1H, chromene C−*H*). ^{13}C NMR ($CDCl_3$-*d*) δ 14.1, 22.8, 27.5, 28.6, 31.7, 44.0 (N-hexyl), 18.8 (CH_3), 55.0 ($C(CH_3)_2$), 101.4 (*C*−O), 121.0, 127.1 (=*C*−H), 112.0, 116.5, 129.4, 130.7, 136.0, 150.0 (indoline ring), 115.1, 116.0, 120.2, 124.1, 139.4, 161.2 (chromene ring).

3. RESULTS AND DISCUSSION

As shown in Scheme 1, 1,3,3-trimethyl-2-methyleneindoline was then treated with 1.2 equiv of salicylaldehyde derivatives in anhydrous ethanol at room temperature for 7 h to generate, after flash column chromatography, N-methyl spiropyran derivatives (1 − 3) in moderate yields (1 64%, 2 83%, 3 88%), respectively. The disappearances of the starting materials was monitored by TLC.

Compounds **1** − **3** exhibit characteristic absorption bands in the infrared spectrum at around 2910 − 2920, 1650 − 1653, and 1604 − 1610 cm^{-1} reflecting the alkyl C−H and vinyl and aromatic C−H bond. Also, these compounds show characteristic C=Caromatic, C=Cvinyl, C−N, and C−O vibration absorption bands in the infrared spectrum at around 1270 and 1090 cm^{-1}. The ^{1}HNMR spectra of **1** − **3** show resonances at around δ = 1.38 – 2.87 ppm due to the methyl proton in the $-CH_3$ and $N-CH_3$ unit and at around δ = 6.00–6.85 ppm due to the vinyl proton in the = C−H unit. The ^{13}C NMR spectra of **1** − **3** exhibit resonances at around δ = 18.0 – 18.7 ($-CH_3$), 30.1–30.5 ($N-CH_3$), 121.1–127.4 (=*C*H), 103.7 – 104.1 (O*C*), and 112.9 – 167.1 ppm (aromatic rings).

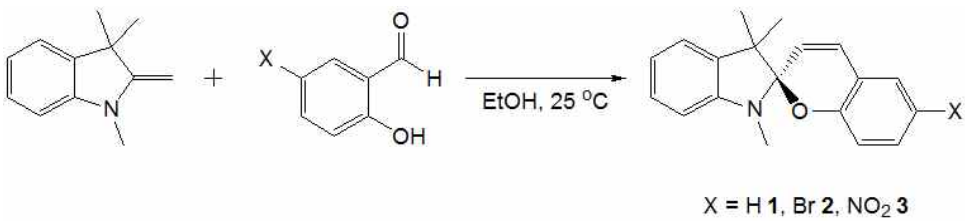

Scheme 1. Synthesis of spiropyrane derivatives **1** − **3.**

As shown in Scheme 2, the starting 5-bromo-2,3,3-trimethyl-3H-indole was prepared by reacting 4-bromo-phenyl hydrazine hydrochloride with 3-methylbutan-2-one under reflux for 8 h in acetonitrile. Upon completion of the reaction, the mixture was cooled to room temperature, and then most of the solvent was evaporated in vacuo. The crude compound was purified by flash column chromatography. 2,3,3-Trimethyl-3H-inodole and iodohexane were dissolved in acetonitrile and heated at reflux for 12 h under a nitrogen atmosphere.

The mixture was cooled to room temperature and then most of the solvent was removed in rotary evaporator. The residue was recrystallized from acetone to afford 2,3,3-trimethyl-1-(3-hexyl)-3H-indolium derivatives. 2,3,3-Trimethyl-1-(3-hexyl)-3H-indolium derivatives and corresponding substituted salicylic aldehydes were dissolved in EtOH and heated at reflux for 24 h under a nitrogen atmosphere. The mixture was cooled to room temperature, and the precipitate was collected by vacuum filtration. The crude product was washed with diethyl ether, and the pure product was purified by flash column chromatography (eluent) **4 – 6.**

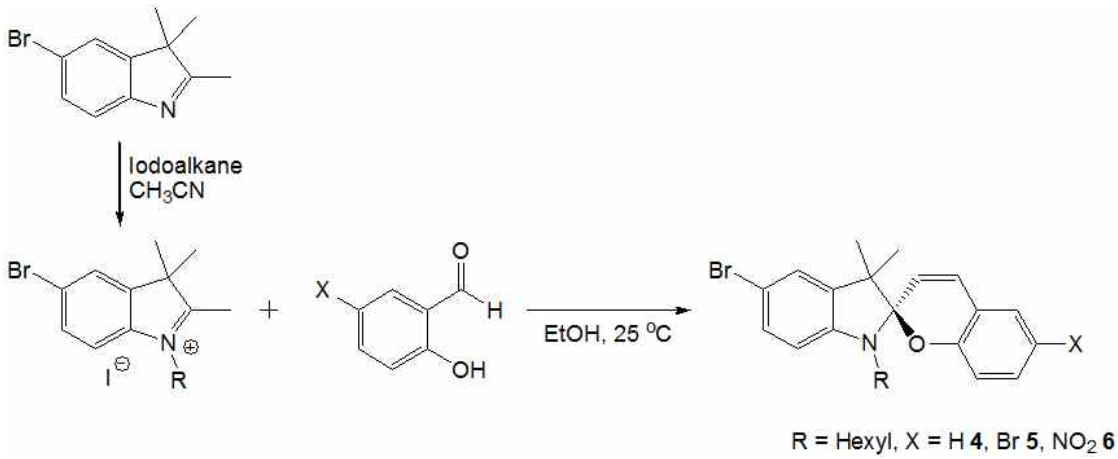

Scheme 2. Synthesis of N-alkylated spiropyran derivatives **4 – 6.**

3.1. Optical Analysis

We investigated six candidates with diversity in the incorporation number of the spiropyran derivatives (Scheme 1 and 2). The designed N-alkylated spiropyran derivatives were synthesized, and their photoisomerization was examined by optical analyses (Figure 1). After irradiation with UV light (360 nm), the spiropyran component of all six candidates converted to the open form, which exhibits absorbance at 540 nm (Figure 1b and 1c, solid lines). Conversely, irradiation with visible light (520 nm) converted the candidate compounds to the closed form, resulting in the disappearance of absorbance at 540 nm (Figure 1b and 1c, dashed lines). These optical changes were confirmed to be reversible,

indicating that the direction of the photoisomerization of spiropyran derivatives can be repeatedly switched by the two wavelengths.

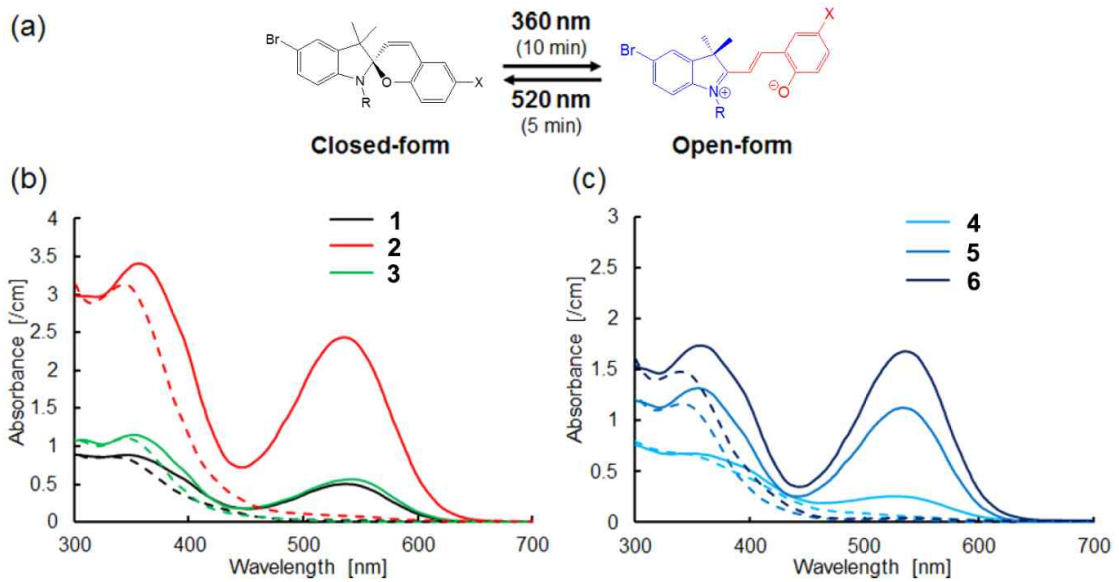

Figure 1. Optical analylsis of synthesized N-alkylated spiropyran derivatives. (a) Schematic of photoisomerization. (b and c) Absorption spectra of spiropyran derivatives. Solid lines: open form, dashed lines: closed form (R = Me, X = H **1**, Br **2**, NO_2 **3**; R = Hx, X = H **4**, Br **5**, NO_2 **6**)

3.2. Photoresponsive Cell Immobilization Assay

The cell-immobilizing ability of the spiropyran derivatives was evaluated in their closed- and open-ring systems by light (UV or visible) irradiation (Figure 2). Non-adherent Ba/F3 cells from the murine pro-B cell line were used, and the cell suspension was added to the modified substrate and washed away after 10 min of incubation. The density of the immobilized cells was determined from microscopic images. The relative cell density compared with that obtained with compound **1** was used to determine cell-immobilizing ability. Compound **1**, some differences in relative cell density were observed between the open and closed form as expected (Figure 2a). However, the on/off ratio was not ideal

because cell immobilization occurred in the “off” state. Consequently, this was thought to be caused by insufficient molecular hydrophobicity even in the ring-closed structure, such that hydrophobic assemblies might not have been sufficiently formed. Compound **2**, with further reduced hydrophobicity, drastically worsened, losing the desired “off” state (Figure 2b). Compound **3**, with moderate hydrophobicity, showed differing cell-immobilizing ability in response to light irradiation and molecular density, which was partially consistent with our working hypothesis (Figure 2c). However, this compound did not also achieve a clear on/off ratio as desired.

Three N-hexylated spiropyran derivatives, compounds **4**, **5**, and **6**, were prepared to increase the hydrophobicity of the closed form. Here, to estimate the hydrophobicity of the compounds, we focused on their log *P* values, which is one of the indicators of hydrophobicity. The theoretically calculated log *P* values[39] in their closed and open forms are listed in Table 1. Compared to the log *P* value of the prototype compound **1**, those of the second-generation compounds were confirmed to be clearly larger. These new candidates exhibited different behaviors in the cell-immobilizing experiments (Figure 2d−f). As shown in Table 1, this result is also explained by the hydrophobicity, which was shown to be the highest among the candidate compounds from the calculated log *P* values. Contrary to compound **1**, the too high molecular hydrophobicity might lead to hydrophobic assembly formation even in the ring-open structure. Compound **4** showed a good on/off ratio (Figure 2d); however, the “off” state slightly worsened, probably because of decreased molecular hydrophobicity. Compound **5**, with similarly moderate hydrophobicity, yielded a very good on/off ratio (Figure 2e). In the “off” state, cell immobilization was suppressed, while cells were immobilized in the “on” state. Compound **6** did not immobilize cells in either the open or closed form (Figure 2f).

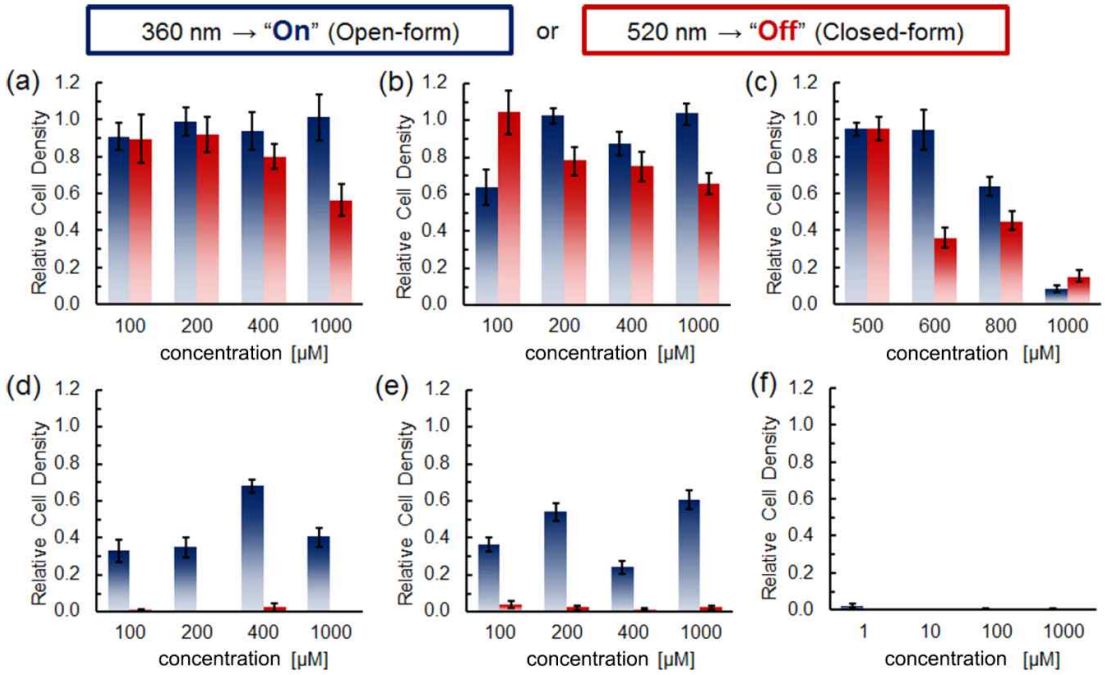

Figure 2. Relative cell densities on the substrate surface modified with compound (a) compound **1,** (b) compound **2,** (c) compound **3,** (d) compound **4,** (e) compound **5,** and (f) compound **6.** Cell density values for the hydrophilic ring-opened form ("on" state) and the hydrophobic ring-closed form ("off" state) are indicated by the blue and red bars, respectively. Cell suspensions in PBS were used in this experiment. Values are the means ± standard error.

This result is also explained by the hydrophobicity, which was shown to be the highest among the candidate compounds from the calculated log *P* values (Table 1). Contrary to compound **1**, the too high molecular hydrophobicity might lead to hydrophobic assembly formation even in the ring-open structure.

Table 1. Predicted log P Values of Spiropyran of **1** – **6**[a]

No.	closed form	open form
1	10.00	8.37
2	11.16	9.69
3	11.21	9.79
4	10.56	8.97
5	10.85	9.33
6	12.87	10.90

[a]The predicted chemical structures are shown in Chart 1. The optical analysis data (Figure 1, the maximum absorption wavelength: 536 nm) clearly showed that the open form was the main form.

From these results so far, we concluded that compounds **4** and **5** are optimal for photo-switchable cell-immobilization, as it exhibited good on/off responsiveness. In addition, those were found that most of the spiropyran derivatives with the log *P* values above 10.5 suppressed cell immobilization in their closed and open forms (Table 1 and Figure 2). Accordingly, the calculated log *P* value of 10.5 might be used as the boundary value for roughly estimating cell immobilization and release. This result suggests that cell-immobilizing ability can be controlled mainly by the strength of the hydrophobicity, although it may be also affected by other factors such as the isomerization efficiency which depended on the substituents of the dye.[40]

3.3. Cytotoxicity Evaluation

Cytotoxic effects of the **3**, **4**, **5**, and **6** on the growth of C6 rat glioma cells were evaluated using an MTT assay. Cell viability after treatment with **5** and **6** at the maximum concentration of 0.1 μM for 2 h remained over 80 and 63%, respectively (Figure 3). At higher concentrations, a sudden decrease in cell viability was observed and no difference was found in cellular viability between **3**, **4**, **5**, and **6** ($p > 0.1$). The results demonstrate that N-alkylated spiropyran derivatives have moderate cytotoxicity at low concentration and lay in the region of acceptable domain for in vitro or in vivo studies below 0.1 μM concentration. The inhibitory concentration (IC_{50})valuesfor**3**, **4**, **5**, and **6** were 0.255 ± 0.05 and 0.184 ± 0.03 μM, respectively.

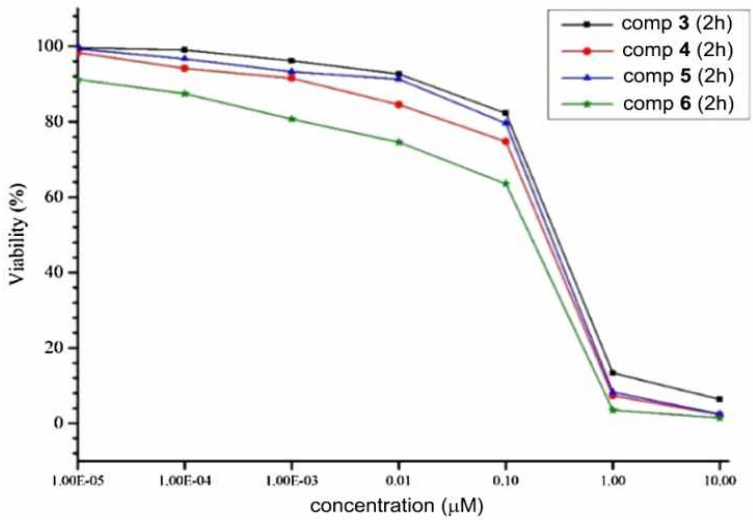

Figure 3. Cytotoxic evaluation of compounds **3**, **4**, **5**, and **6** for C6 rat glioma cells. Viability assay after 2 h incubation at 37 °C for 4 h in the dark.

As shown in Figures 4 and 5, the mitochondrial activity was reduced in a dose-dependent manner after exposure to UV irradiation (365 nm) for 3 min and significant differences was observed between the treated cells with compounds **3**, **4**, **5**, and **6** before and after UV exposure. Obviously, compounds **3**, **4**, **5**, and **6** caused about 1.1−1.2 fold and 1.3−1.7 fold intensification of cell inhibition after UV irradiation, respectively, in comparison with the control samples (not illuminated) at the concentrations of 0.001−0.1 μM for 2 h. As a result, the cell inhibition without UV irradiation greatly depends on cellular uptake of the spiropyrans. After UV irradiation, 26% cell destruction was observed for the treated C6 cells with 0.1 μM compounds **5**and **6** in comparison with non-irradiated ones. This probably refers to the enhanced ROS photo-generation caused by strongly coupled interaction between MC isomers.

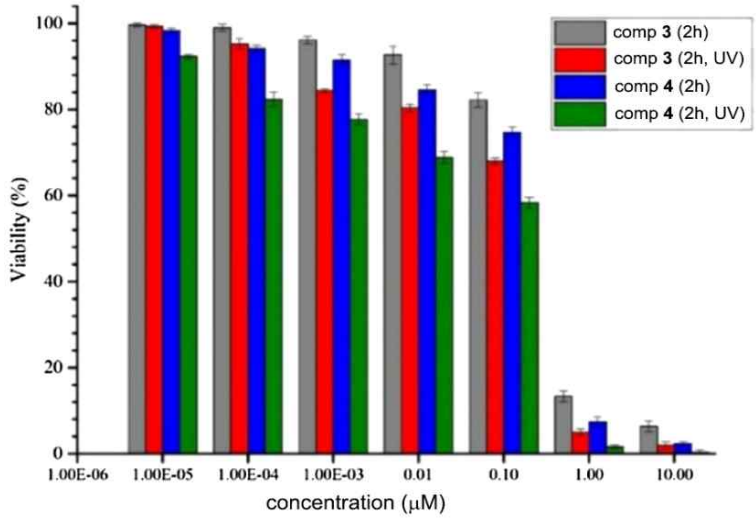

Figure 4. Cytotoxic evaluation of **3** and **4** for C6 rat glioma cells. Viability assay after 2 h incubation and subsequent 3 min UV irradiation at 365 nm.

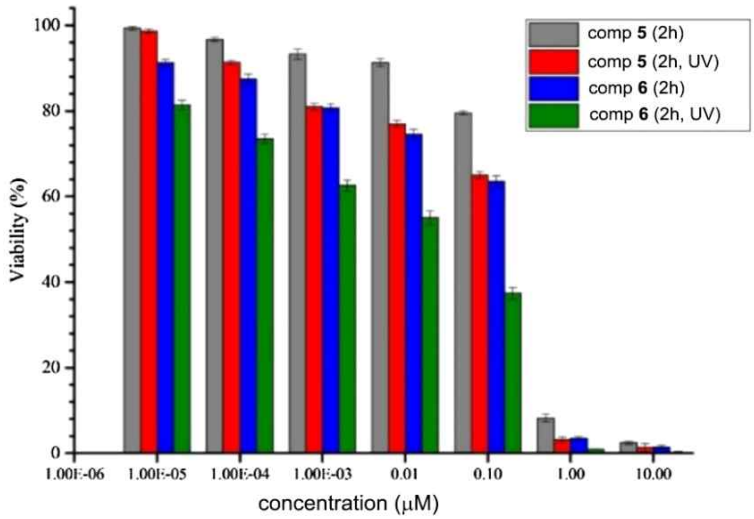

Figure 5. Cytotoxic evaluation of **5** and **6** for C6 rat glioma cells. Viability assay after 2 h incubation and subsequent 3 min UV irradiation at 365 nm.

3.4. Intracellular ROS Detection and Analysis.

Generation of intracellular ROS can be detected by the oxidation-sensitive dye, DCFH, as a fluorescent probe. In the presence of ROS, the trapped non-fluorescent DCFH inside the

cells is rapidly oxidized to highly fluorescent dichlorofluorescein (DCF) with emission at 528 nm that is directly proportional to the extent of generated ROS. It is noteworthy that none of **SP** or **MC** moieties have fluorescence emission at this wavelength. The DCF assay can detect all kinds of ROS and is considered as a reliable method for evaluating photo-cytotoxicity.[41-44] Therefore, extra fluorescence emission of DCF, caused by the presence of compounds **3** and **6**, can be ascribed to the photo-generation of cytotoxic ROS. By green light illumination at 532 nm, the valence electrons in the prepared N-alkylated spiropyran derivatives can absorb energy and excite from the singlet ground state (S_0)tothesingletexcitedstate(S_1)(Figure6).

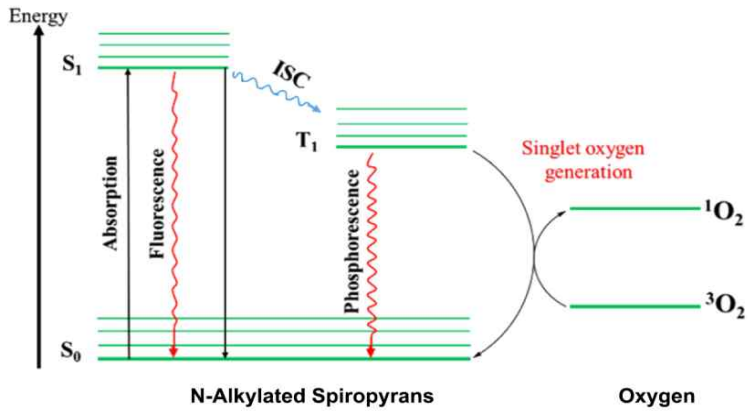

Figure 6. Energy diagram for MC resonance coupling in singlet oxygen generation.

Then, S_1 may reach to the triplet excited state (T_1) by ISC and this subsequently leads to the transforming of the ground state molecular oxygen ($^3O_2$) to the singlet oxygen ($^1O_2$) through energy transfer from T_1s tate of spiropyrans. Figure7 shows the variations in fluorescence intensity within each 1 min interval and during 5 min in the presence of compounds **3** and **6**, with and without UV irradiation for 3 min (365 nm) and subsequent green light exposure (532 nm). Without UV irradiation, compound **6** demonstrated more fluorescence emission in comparison with compound **3**, which indicates highly localized plasmonic field and more concentration and accumulation of compound **6** in the C6 glioma cells.

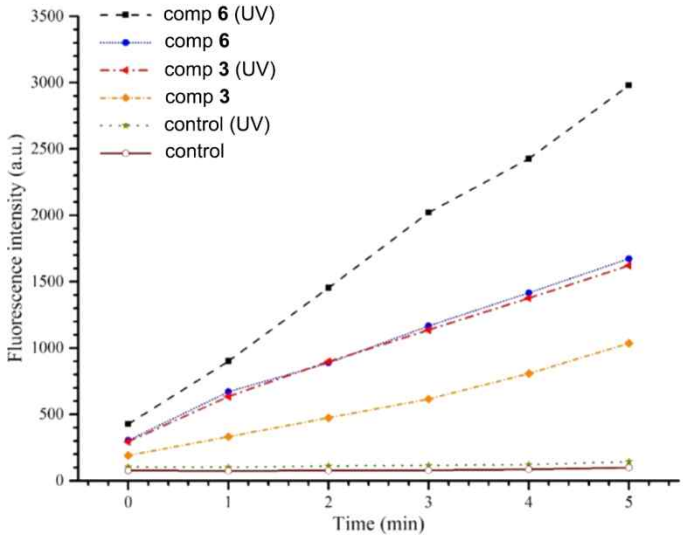

Figure 7. Fluorescence emission intensity of DCF at 528 nm vs time, with and without UV irradiation (365 nm, 3 min) in C6 glioma cells for the control sample and in the presence of 0.01 μM compounds **3** and **6**.

The fluorescence intensity of DCF increased with a higher slope for those including compound **6** after UV irradiation than the others, which depicts the generation of more ROS there. Also after 3 min of UV irradiation, 1.56- and 1.83-fold increase in fluorescence emission was observed for compounds **3** and **6**, respectively, relative to the samples without UV irradiation. Photo-generated intracellular ROS like singlet oxygen will increase biological damages in the exposed cells via gold-enhanced singlet oxygen photogeneration.[45,46] This improvement in ROS generation can be attributed to the enhanced interaction between dipolar moment of zwitterionic MC. Results of intracellular ROS analysis demonstrate that compound **6** with the enhanced ROS generation are a good candidate for selective targeted photodynamic therapy in cancer cells.

4. Conclusion

N-Alkylated spiropyran derivatives were designed and synthesized, and the compounds **4** and **5**, which showed the good performance, enabled the reversible immobilization of three types of model cells without the need for their inherent cellular adhesion. Furthermore, UV−vis analysis showed that the absorption band of MC isomer (λ_{max}=565nm) and this resulted in their efficient dipolar interactions and led to 10 nm in SPR red shift. The MTT assay revealed increment in cell destruction of the treated C6 rat glioma cancer cells with spiropyran derivatives under UV irradiation at 365nm. On the other hand, the compounds **3** and **6** induced enhanced generation of ROS, as an efficient method for cell death and cancer therapy.

5. References

[1] H. M. D. Bandara, S. C. Burdette, *Chem. Soc. Rev.* **2012**, *41*, 1809–1825.

[2] J. Broichhagen, J. A. Frank, D. Trauner, *Acc. Chem. Res.* **2015**, *48*, 1947–1960.

[3] L. Laprell, E. Repak, V. Franckevicius, F. Hartrampf, J. Terhag, M. Hollmann, M. Sumser, N. Rebola, D. A. DiGregorio, D. Trauner, *Nat. Commun.* **2015**, *6*, 1–11.

[4] R. Göstl, A. Senf, S. Hecht, *Chem. Soc. Rev.* **2014**, *43*, 1982–1996.

[5] S. Steinwand, T. Halbritter, D. Rastädter, J. M. Ortiz-Sánchez, I. Burghardt, A. Heckel, J. Wachtveitl, *Chem. Eur. J.* **2015**, *21*, 15720–15731.

[6] M. Stein, S. J. Middendorp, V. Carta, E. Pejo, D. E. Raines, S. A. Forman, E. Sigel, D. Trauner, *Angew. Chem. Int. Ed.* **2012**, *51*, 10500–10504.

[7] J. Wachtveitl, T. Nägele, B. Puell, W. Zinth, M. Krüger, S. Rudolph-Böhner, D. Oesterhelt, L. Moroder, *J. Photochem. Photobiol. Chem.* **1997**, *105*, 283–288.

[8] H. Satzger, S. Spörlein, C. Root, J. Wachtveitl, W. Zinth, P. Gilch, *Chem. Phys. Lett.* **2003**, *372*, 216–223.

[9] V. I. Minkin, *Chem. Rev.* **2004**, *104*, 2751–2776.

[10] J. Buback, M. Kullmann, F. Langhojer, P. Nürnberger, R. Schmidt, F. Würthner, T. Brixner, *J. Am. Chem. Soc.* **2010**, *132*, 16510–16519.

[11] H. Görner, *Phys. Chem. Chem. Phys.* **2001**, *3*, 416–423.

[12] N. P. Ernsting, T. Arthen-Engeland, *J. Phys. Chem.* **1991**, *95*, 5502–5509.

[13] M. Irie, *Chem. Rev.* **2000**, *100*, 1685–1716.

[14] Y. Yokoyama, Y. Kurita, *Mol. Cryst. Liq. Cryst. Sci. Technol. A. Mol. Cryst. Liq. Cryst.* **1994**, *246*, 87–94.

[15] S. Draxler, T. Brust, S. Malkmus, J. A. DiGirolamo, W. J. Lees, W. Zinth, M. Braun, *Phys. Chem. Chem. Phys.* **2009**, *11*, 5019–5027.

[16] C. Slavov, N. Bellakbil, J. Wahl, K. Mayer, K. Rück-Braun, I. Burghardt, J. Wachtveitl, M. Braun, *Phys. Chem. Chem. Phys.* **2015**, *17*, 14045–14053.

[17] B. Heinz, S. Malkmus, S. Laimgruber, S. Dietrich, C. Schulz, K. Rück-Braun, M. Braun, W. Zinth, P. Gilch, *J. Am. Chem. Soc.* **2007**, *129*, 8577–8584.

[18] C. Slavov, C. Boumrifak, C. A. Hammer, P. Trojanowski, X. Chen, W. J. Lees, J. Wachtveitl, M. Braun, *Phys*. *Chem*. *Chem*. *Phys*. **2016**, *18*, 10289–10296.

[19] R. Klajn, *Chem*. *Soc*. *Rev*. **2014**, *43*, 148–184.

[20] D. Davis, A. Hamilton, J. Yang, L. D. Cremar, D. Van Gough, S. L. Potisek, M. T. Ong, P. V. Braun, T. J. Martínez, S. R. White, J. S. Moore, N. R. Sottos, *Nature* **2009**, *459*, 68–72.

[21] T. Sendai, S. Biswas, T. Aida, *J. Am*. *Chem*. *Soc*. **2013**, *135*, 11509–11512.

[22] M. Kullmann, S. Ruetzel, J. Buback, P. Nürnberger, T. Brixner, *J. Am*. *Chem*. *Soc*. **2011**, *133*, 13074–13080.

[23] J. Hobley, V. Malatesta, R. Millini, L. Montanari, Jr. W. O Neil Parker, *Phys*. *Chem*. *Chem*. *Phys*. **1999**, *1*, 3259–3267.

[24] A. K. Chibisov, H. Görner, *J. Phys*. *Chem*. **1997**, *101*, 4305–4312.

[25] I. Gómez, M. Reguero, M. A. Robb, *J. Phys*. *Chem*. *A* **2006**, *110*, 3986–3991.

[26] C. Walter, S. Ruetzel, M. Diekmann, P. Nürnberger, T. Brixner, B. Engels, *J. Chem*. *Phys*. **2014**, *140*, 224311.

[27] S. Prager, I. Burghardt, A. Dreuw, *J. Phys*. *Chem*. *A* **2014**, *118*, 1339–1349.

[28] D. D. Young, A. Deiters, *ChemBioChem* **2008**, *9*, 1225–1228.

[29] C. Brieke, A. Heckel, *Chem*. *Eur*. *J*. **2013**, *19*, 15726–15734.

[30] M. Bälter, M. Hammarson, P. Remón, S. Li, N. Gale, T. Brown, J. Andréasson, *J. Am*. *Chem*. *Soc*. **2015**, *137*, 2444–2447.

[31] J. Andersson, S. Li, P. Lincoln, J. Andréasson, *J. Am*. *Chem*. *Soc*. **2008**, *130*, 11836–11837.

[32] A. Koçer, M. Walko, B. L. Feringa, *Nat*. *Protoc*. **2007**, *2*, 1426–1437.

[33] T. Stafforst, D. Hilvert, *Chem*. *Commun*. *Camb*. *Engl*. **2009**, 287–288.

[34] M. Hammarson, J. R. Nilsson, S. Li, T. Beke-Somfai, J. Andréasson, *J. Phys*. *Chem*. *B* **2013**, *117*, 13561–13571.

[35] D. Movia, A. Prina-Mello, Y. Volkov, S. Giordani, *Chem*. *Res*. *Toxicol*. **2010**, *23*, 1459–1466.

[36] H.-A. Wagenknecht, C. Beyer, *Synlett* **2010**, *9*, 1371–1376.

[37] S. R. Keum, K. B. Lee, P. M. Kazmaier, E. Buncel, Tetrahedron Lett. 1994, 35, 1015–1018.

[38] C. Wang, Q. Cui, X. Wang, L. Li, *ACS Appl. Mater. Interfaces* **2016**, *8*, 29101−29109.

[39] I. V. Tetko, J. Gasteiger, R. Todeschini, A. Mauri, D. Livingstone, P. Ertl, V. A. Palyulin, E. V. Radchenko, N. S. Zefirov, A. S. Makarenko, V. Y. Tanchuk, W. Prokopenko, *J. Comput. Aided Mol. Des*. **2005**, *19*, 453−463.

[40] R. Klajn, *Chem. Soc. Rev*. **2014**, *43*, 148−184.

[41] B. Wang, J.-H. Wang, Q. Liu, H. Huang, M. Chen, K. Li, C. Li, X.-F. Yu, P. K. Chu, *Biomaterials* **2014**, *35*, 1954−1966.

[42] C. Wang, Q. Cui, X. Wang, L. Li, *ACS Appl. Mater. Interfaces* **2016**, *8*, 29101−29109.

[43] J. Xu, P. Yang, M. Sun, H. Bi, B. Liu, D. Yang, S. Gai, F. He, J. Lin, *ACS Nano* **2017**, *11*, 4133−4144.

[44] S. Li, K. Chang, K. Sun, Y. Tang, N. Cui, Y. Wang, W. Qin, H. Xu, C. Wu, *ACS Appl. Mater. Interfaces* **2015**, *8*, 3624−3634.

[45] Y. Li, T. Wen, R. Zhao, X. Liu, T. Ji, H. Wang, X. Shi, J. Shi, J. Wei, Y. Zhao, X. Wu, G. Nie, *ACS Nano* **2014**, *8*, 11529−11542.

[46] Y. Zhang, K. Aslan, M. J. R. Previte, C. D. Geddes, *Proc. Natl. Acad. Sci. U.S.A*. **2008**, *105*, 1798−1802.